Investigation of the Structural Stability of the Human Acidic Fibroblast Growth Factor by Hydrogen−Deuterium Exchange[†]

Ya-Hui Chi,[‡] Thallampuranam Krishnaswamy S. Kumar,[‡] Karuppanan Muthusamy Kathir,[‡] Dong-Hai Lin,[§] Guang Zhu,[§] Ing-Ming Chiu,[⊥] and Chin Yu*,[‡]

Department of Chemistry, National Tsing Hua University, Hsinchu 30013, Taiwan, Department of Biochemistry, The Hong Kong University of Science, Clear Water Bay, Kowloon, Hong Kong, and Department of Internal Medicine, The Ohio State University, Columbus, Ohio 43210

Received May 30, 2002; Revised Manuscript Received October 6, 2002

ABSTRACT: The conformational stability of the human acidic fibroblast growth factor (hFGF-1) is investigated using amide proton exchange and temperature-dependent chemical shifts, monitored by two-dimensional NMR spectroscopy. The change in free energy of unfolding (ΔG_u) of hFGF-1 is estimated to be 5.00 ± 0.09 kcal·mol^{-1}. Amide proton-exchange rates of 74 residues (in hFGF-1) have been unambiguously measured, and the exchange process occurs predominately according to the conditions of the EX2 limit. The exchange rates of the fast-exchanging amide protons exposed to the solvent have been measured using the clean SEA-HSQC technique. The amide proton protection factor and temperature coefficient estimates show reasonably good correlation. Residues in β-strands II and VI appear to constitute the stability core of the protein. Among the 12 β-strands constituting the β-barrel architecture of hFGF-1, β-strand XI, located in the heparin binding domain, exhibits the lowest average protection factor value. Amide protons involved in the putative folding nucleation site in hFGF-1, identified by quench-flow NMR studies, do not represent the slow-exchanging core. Residues in portions of hFGF-1 experiencing high conformational flexibility mostly correspond to those involved in receptor recognition and binding.

Proteins are dynamic and not static systems (*1*). Proteins often undergo conformational changes to execute their biological functions, such as an enzyme reaction or ligand binding (*2*). Internal protein dynamics can potentially affect protein function through a variety of mechanisms, and there are now several examples of protein−protein and protein−ligand interactions that illustrate that dynamics may be intricately linked to function in several ways (*3*−*7*). In this context, the static three-dimensional structures which provide a description of the ground state of the molecule alone cannot explain the results from functional biological assays (*8*). As macromolecular function(s) is dependent on excursion to excited molecular states, a comprehensive understanding of the intramolecular dynamical modes in protein demands characterization of the energetics and mechanisms of motions as well as the time scales and amplitudes (*9*−*12*).

Hydrogen−deuterium (H/D[1])-exchange kinetics (*13*−*15*) and ^{15}N spin relaxation (*16*), monitored by nuclear magnetic resonance spectroscopy, are powerful tools to study protein dynamics in relation to protein functions. These two techniques, put together, can report internal motions occurring in the milli- to submillisecond time regime (*1*). In particular, amide proton-exchange measurements could be extended to obtain valuable information on the free energy relationships underlying fundamental units of protein structure (*17*−*20*). In addition, as the H/D-exchange measurements can be made in the absence of denaturants, they are not plagued by the uncertainties and difficulties often encountered (in the estimation of thermodynamic parameters) at extreme denaturing conditions (*21*).

Amide protons involved in backbone hydrogen bonds are proposed to exchange with the solvent according to the following scheme (*22*, *23*):

$$\text{closed} \underset{k_{cl}}{\overset{k_{op}}{\rightleftharpoons}} \text{open} \xrightarrow{k_{rc}} \text{exchanged}$$

where k_{op} is the rate of opening, k_{cl} is the rate of closing, and k_{rc} is the intrinsic exchange rate of the protein. Under native conditions, there is an equilibrium preceding chemical exchange, with the open conformation being susceptible to exchange. This behavior is described by the equation $k_{ex} = k_{op}k_{rc}/(k_{cl} + k_{rc})$, where k_{ex} is the observed rate of exchange. In the usual kinetic limit, known as the EX2 condition, where structural reclosing is faster than the intrinsic unprotected exchange rate ($k_{cl} \gg k_{rc}$), the hydrogen-exchange rate measured for any given hydrogen (k_{ex}) provides the transient opening equilibrium constant ($K = k_{ex}/k_{rc}$). The free energy of the determined opening reaction can be calculated as $\Delta G_{ex} = -RT \ln K$ (*24*). Therefore, the measurement of hydrogen-exchange rates can provide site-specific information on the presence or absence of H-bond structure and its stability, dynamics, and other properties (*25*, *26*).

[†] This work was supported by the National Science Council, Taiwan.

* To whom correspondence should be addressed. Fax: 886-3-5711082. E-mail: cyu@mx.nthu.edu.tw.

[‡] National Tsing Hua University.

[§] The Hong Kong University of Science.

[⊥] The Ohio State University.

[1] Abbreviations used: CD, circular dichroism; HSQC, heteronuclear single quantum coherence; H/D, hydrogen−deuterium; NOE, nuclear Overhauser effect; RNase, ribonuclease; SEA, solvent-exposed amides.

10.1021/bi026218a CCC: $22.00
Published on Web 11/27/2002

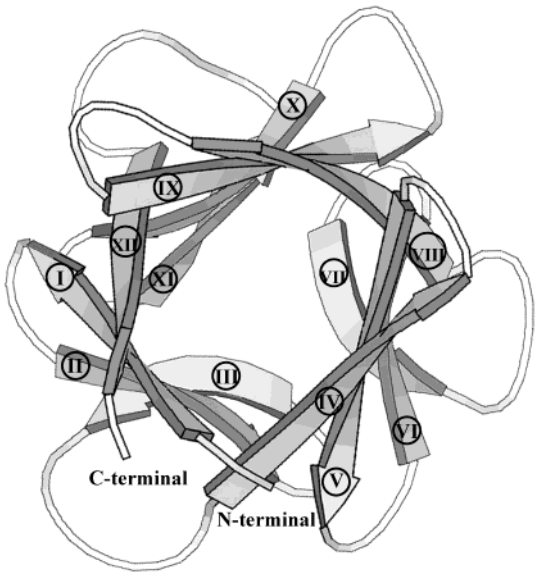

FIGURE 1: MOLSCRIPT representation of the structure hFGF-1. The secondary structural elements in the protein include 12 β-strands arrayed into a β-barrel architecture. The circled numbers in the figure indicate the individual β-strands in the protein.

Human acidic fibroblast growth factor (hFGF-1, $M_r \approx 16$ kDa) plays crucial roles in key biological processes such as cell growth, angiogenesies, and wound healing (*27*−*30*). High-resolution crystal and solution structures of hFGF-1 show that it is an all β-sheet protein with 12 β-strands arranged into a β-barrel architecture (Figure 1; *31*−*35*). In the present study, we investigate the conformational stability and dynamics of hFGF-1 on the basis of amide proton-exchange kinetics and temperature coefficient (*36*) measurements monitored by NMR spectroscopy.

MATERIALS AND METHODS

Heparin-Sepharose was obtained from Amersham Pharmacia Biotech. Labeled $^{15}NH_4Cl$ and D_2O were purchased from Cambridge Isotope Laboratories. Urea-d_4 was purchased from Sigma. All other chemicals used were of high-quality analytical grade. All experiments were performed at 25 °C.

Equilibrium Unfolding. Urea-induced unfolding of hFGF-1 was performed using fluorescence spectroscopy on a Hitachi F-2500 spectrofluorometer at 2.5-nm resolution, using an excitation wavelength of 280 nm. A 25 μg/mL concentration of hFGF-1 in 100 mM phosphate buffer (pH/pD 6.0) in H_2O/D_2O containing 200 mM ammonium sulfate was used for the unfolding experiments.

Expression and Purification of ^{15}N-Labeled hFGF-1. Residues are numbered according to their position in the primary structure of the 154-amino-acid hFGF-1. The expression vector for the truncated form of the human FGF-1 (hFGF-1, residues 15−154) was constructed and inserted between the *Nde*I and *Bam*HI restriction sites in pET20b-(+). *Escherichia coli* BL21(DE3)pLysS, harboring pET20b-(+)-hFGF-1, was cultured in minimal medium containing $^{15}NH_4Cl$. Recombinant protein was purified on heparin-Sepharose using a gradient (0−1.5 M NaCl). Protein expression yields were in the range of 25−30 mg/L. The extent of ^{15}N labeling was verified by electron spray−mass analysis.

Measuring Temperature Coefficient. ^{15}N-Labeled hFGF-1 was prepared in 10% D_2O/90% H_2O in 100 mM phosphate buffer and 100 mM ammonium sulfate at pH 6.5. The sample was concentrated to ∼1.5 mM by a centricon (Millipore). All spectra were acquired on a Bruker DMX-600 spectrometer. Spectra were recorded with 16 transients of 2048 data points and 128 t_1 increments. For the determination of the NH temperature coefficient, $^1H-^{15}N$ HSQC spectra were recorded from 288.5 to 306 K at 2.5 K intervals. The probe temperature was calibrated by measuring the peak separation (in ppm) between the OH and CH_3 resonances in 100% methanol. Proton chemical shifts were referenced to 3-trimethylsilylpropionate-*2,2,3,3-d*$_4$ sodium salt (TSP), and ^{15}N chemical shifts were referenced using the consensus ratio of 0.0101329118. All spectra were processed on a Silicon Graphics workstation using UXNMR, AURELIA, and SPARKY software.

Measuring Amide Proton-Exchange Rate. Protein solution was prepared in 100 mM phosphate buffer and 200 mM ammonium sulfate at pH 6.0 and pH 7.0. The sample was concentrated to ∼1.5 mM by ultrafiltration (Millipore) and dried by lyophilization. H/D exchange was initiated by dissolving dry protein in 10 mM phosphate-buffered D_2O at pD 6.0 and pD 7.0 (at 25 °C), respectively. All NMR data acquisition parameters were preset using a mock sample, and sample pH was measured after the experiment to minimize the dead time. The first $^1H-^{15}N$ HSQC spectrum was acquired after 8 min of initiation of exchanges. Spectra were recorded with 8 transients of 2048 data points and 64 t_1 increments. Fifty spectra were collected in 48 h with various time points, and another eight spectra were collected in 1265 h.

Amide Proton-Exchange Analysis. The peak heights in the two-dimensional spectra were measured using the peak-picking subroutine and referenced internally to a non-exchangeable resonance aliphatic proton in one-dimensional ^{1}H spectra. To determine rate constants for exchange, NH resonance intensities (I) as a function time (t) were fit to a single-exponential function, $I = I_o \exp(-k_{ex}t) + C$, where I_o is the initial intensity, k_{ex} is the rate constant of exchange, and C is the final amplitude. The protection factors (P) for the various amide protons in the protein were estimated on the basis of the method reported by Bai et al. (*24*), using the equation $P = k_{rc}/k_{ex}$, where k_{rc} and k_{ex} represent the exchange rates of the protein in the random coil and native conformations states, respectively. As reported by Bai et al. (*24*), the hydrogen-exchange rates of amide protons in nonstructured peptides, termed k_{rc}, are estimated by referencing an alanine-based peptide (poly-DL-alanine, PDLA) at low ionic strengths at 20 °C. The free energy of exchange of the amide protons was calculated from the equation $\Delta G_{ex} = -RT \ln(k_{ex}/k_{rc})$, where R is the gas constant and T is the absolute temperature at which the exchange was monitored.

Clean SEA-HSQC Experiments. Clean SEA-HSQC experiments were performed on a 1.0 mM uniformly ^{15}N-labeled sample of hFGF-1 in 100 mM phosphate buffer and 200 mM ammonium sulfate in 90% H_2O/10% D_2O at pH 6.0 (37). All the two-dimensional NMR experiments were performed on a Varian Unity INOVA 750 MHz spectrometer at 25 °C. The mixing times (τ_m) used for the experiments were 20, 35, 50, 75, 100, and 150 ms. The prescan delay was 2.0 s, and each spectrum was collected with 128 transients of 2048 real points and 256 t_1 increments. The peak heights in the two-dimensional $^1H-^{15}N$ HSQC spectra were measured

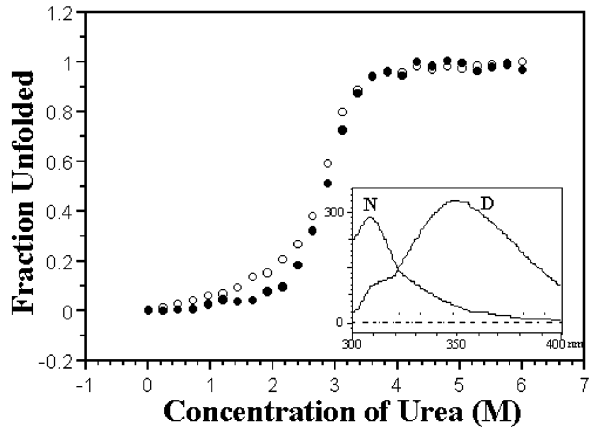

FIGURE 2: Urea-induced equilibrium unfolding of hFGF-1 in H_2O (○) and in D_2O (●). The stability of the protein is observed to increase marginally in D_2O. The unfolding profile was generated by monitoring the 350/308-nm fluorescence changes in the protein [in 100 mM phosphate buffer (pH/pD) 6.0 containing 200 mM ammonium sulfate at 25 °C]. The inset shows the fluorescence spectra of hFGF-1 in the native (N) and denatured (D) states.

using the peak-picking subroutine. To determine rate constants for exchange, NH resonance intensities (S) as a function of mixing time (τ_m) were fit to an exponential function (*38*), $S/S_{ref} = [k_{ex}/(R_{1A} + k_{ex} - R_{1B})]\{\exp(-R_{1B}\tau_m) - \exp[-(R_{1A} + k_{ex})]\tau_m\}$, where S_{ref} is the reference peak intensity in the normal $^1H-^{15}N$ gradient-enhanced HSQC spectrum, k_{ex} is the H/D-exchange rate constant, R_{1A} is the combination of longitudinal relaxation and transverse relaxation rates of amide protons, and R_{1B} is that of water molecules.

RESULTS AND DISCUSSION

Equilibrium Unfolding of hFGF-1. The fluorescence spectrum of hFGF-1 in the native conformation shows an emission maximum around 308 nm (Figure 2, inset). The fluorescence of the lone tryptophan residue located at position 121 of the amino acid sequence is completely quenched in the native state of the protein (*30*, *39*, *40*). The quenching effect is attributed to the presence of imidazole and pyrrole groups in close proximity to the indole side chain of Trp121 in the three-dimensional structure of hFGF-1 (*33*, *40*). However, the quenching effect is relieved upon unfolding, and the fluorescence spectrum of hFGF-1 in the unfolding state shows an emission maximum around 350 nm (Figure 2, inset; *30*, *39*, *40*). Hence, the conformational changes occurring during the unfolding/refolding of the protein could be reliably studied by monitoring changes in the 350/308-nm fluorescence.

Urea-induced equilibrium unfolding of hFGF-1, monitored by steady-state fluorescence spectroscopy, shows that the protein unfolds reversibly with a C_m (concentration of urea at which 50% of the molecules exist in the unfolded state) of 2.67 ± 0.09 M (Figure 2). The m value, which is a measure of the cooperativity of the unfolding process, is estimated to be 1.60 ± 0.07 kcal·mol^{-1}·M^{-1}. The unfolding profile of hFGF-1, obtained by monitoring the ellipiticity (within experimental error) changes at 228 nm, superimposes well with the unfolding curve derived using steady-state fluorescence (data not shown). This aspect implies that the unfolding of the protein under these conditions follows a two-state (native ↔ unfolded) transition. The free energy [$\Delta G(H_2O)$] change for the unfolding process is estimated to be 4.20 ± 0.07 kcal·mol^{-1}.

Proteins generally exhibit higher stability in D_2O. For this reason, the urea-induced equilibrium unfolding of hFGF-1 was also studied in D_2O. The $\Delta G(D_2O)$ (5.00 ± 0.09 kcal·mol^{-1}) and the C_m (2.79 ± 0.07) values for the unfolding process in D_2O are marginally higher than those in H_2O. The moderate increase in the $\Delta G(D_2O)$ value probably reflects a small increase in the stability of the native conformation of the protein in D_2O. The increase in the conformational stability of the native state (hFGF-1) also appears to increase the cooperativity (m = 1.80 ± 0.02 kcal·mol^{-1}·M^{-1}) of the transition from the native to the unfolded state(s) (Figure 2).

Relationship between H/D Exchange and Structure. The $^1H-^{15}N$ HSQC spectrum of hFGF-1 (at 25 °C) is well-dispersed, and all the cross-peaks have been unambiguously assigned (*29*, *30*, *34*). Total exchange rates of 74 (out of 120 residues) could be unambiguously followed. Forty-six main-chain amide protons exchange out within the first 20 min of initiation of exchange, and most of them correspond to residues located in the unstructured loop regions of the hFGF-1 molecule (Figure 3A, Table 1). In addition, 11 residues exchange very fast, with rate constants (k_{ex}) greater than 1×10^{-2} min^{-1}. Except for Ser61 and Gln77, which are located at the fringe of β-strand IV and β-strand VI, respectively, the remaining six residues, which exhibit very fast rates of exchange ($k_{ex} > 1 \times 10^{-2}$ min^{-1}), are located in the loop regions of the molecule (Table 1). Thirty-seven residues exchange at a moderately fast rate (2×10^{-4} min^{-1} $< k_{ex} < 1 \times 10^{-2}$ min^{-1}). These include many residues located in β-strands III, VII, VIII, IX, X, and XI (Table 1). Eighteen residues exhibit a very slow exchange rate (7×10^{-5} min^{-1} $< k_{ex} < 2 \times 10^{-4}$ min^{-1}). The residues which fall into this category include several residues from β-strands V and XII. Gly85 and Ala143, which are located at the fringe of β-strands VII and XII, respectively, show strong protection against H/D exchange ($k_{ex} \approx 1 \times 10^{-4}$ min^{-1}). There are eight residues which depict extraordinarily high protection ($k_{ex} < 7 \times 10^{-5}$ min^{-1}). These include Arg38, Ile39, and Leu40 (located in β-strand II), Tyr78, Leu79, and Ala80 (constituting β-strand VI), Leu86 (Figure 3B, in β-strand VII), and Leu100 (in β-strand VIII).

The exchange rates ($k_{ex} > 1$ min^{-1}) of the solvent-exposed, rapidly exchanging amide protons in hFGF-1 have been measured using the clean SEA-HSQC technique (*37*). About 41 $^1H-^{15}N$ cross-peaks, corresponding to the solvent-exposed fast exchanging amide protons in hFGF-1, could be observed in the clean SEA-HSQC spectra collected even at a low mixing time of 20 ms (Figure 4A). These cross-peaks correspond to the amide protons of Gln91, Glu118, Lys142, and Ser152 (Figure 4B). Although most of the 46 fast-exchanging amide protons could be detected in the clean SEA-HSQC spectra (obtained with mixing times ranging from 20 to 150 ms), exchange rates of only 18 of these amide protons could be quantitatively estimated (Table 2, Figure 4). Among the fast-exchanging amide protons (in hFGF-1) whose exchange rates could be estimated, the amide proton of Ser153, which is located in the unstructured C-terminal domain, exchanges most rapidly with the solvent ($k_{ex} = 1.43 \times 10^3$ min^{-1}).

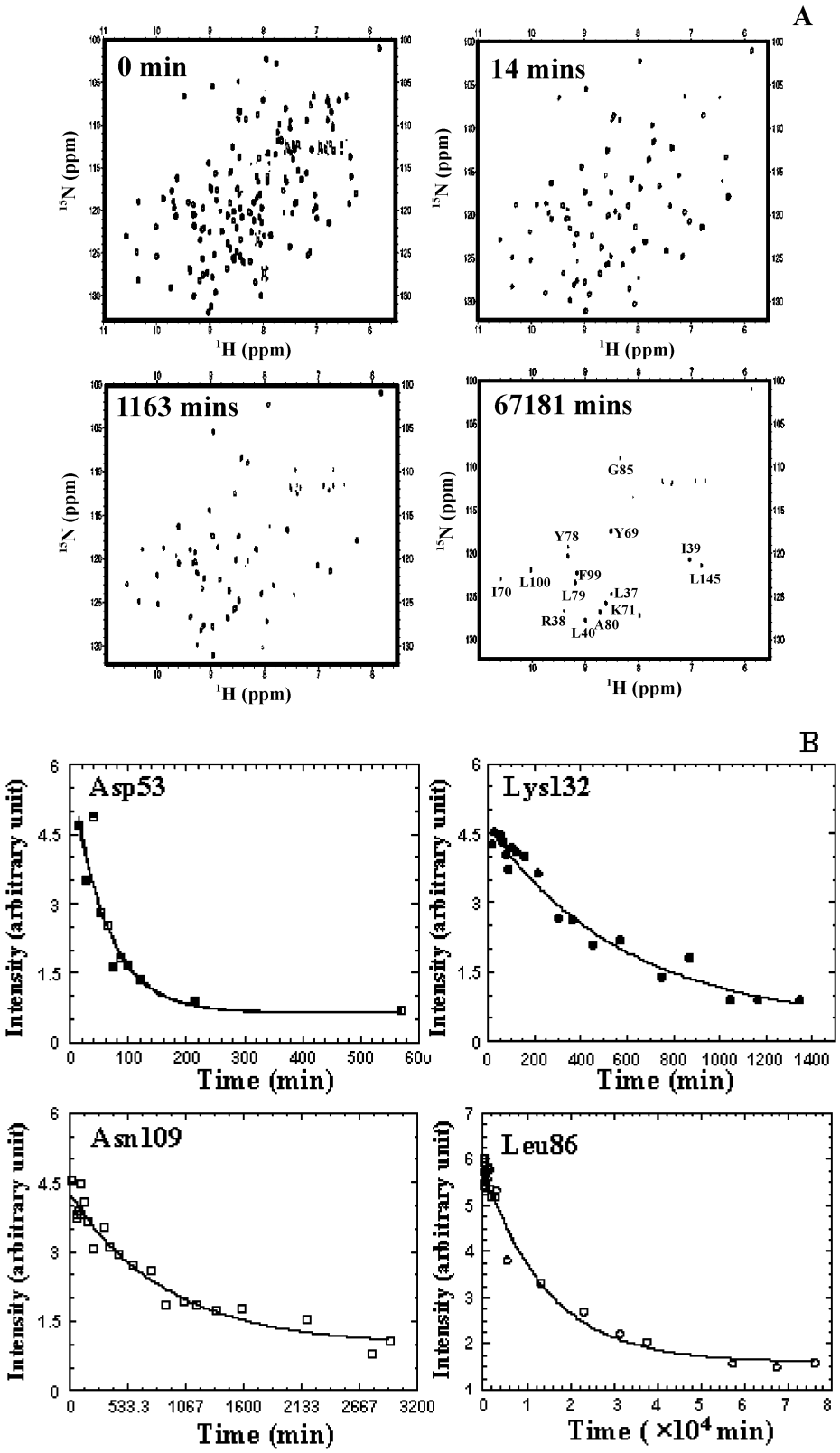

FIGURE 3: (A) ^{1}H−^{15}N HSQC spectra of hFGF-1 after various time periods of exchange in D_2O. (B) Time course of exchange of selected residues in hFGF-1.

The protection factor(s) estimated from hydrogen−deuterium-exchange experiments is a useful and reliable measure to evaluate the degree of protection of an amide proton against H/D exchange (*14*, *20*−*22*). The average protection factors of the 12 β-strands constituting the β-trefoil structure of hFGF-1 decrease in the order of β-strand VI (478 405 ± 68 866) > β-strand II (316 990 ± 29 341) > β-strand VII (123 032 ± 4720) > β-strand V (112 332 ± 3992) > β-strand I (99 707 ± 1637) > β-strand IX (91 743 ± 1704) > β-strand X (64 204 ± 1083) > β-strand III (54 150 ± 1098) > β-strand XII (47 819 ± 3553) > β-strand VIII (43 212 ± 7604) > β-strand IV (29 281 ± 925) >

Table 1: Hydrogen−Deuterium-Exchange Patterns of Residues in hFGF-1

rate constant (k_{ex}) range	residues
$k_{ex} < 7 \times 10^{-5}$ min^{-1}	R38, I39, L40, Y78, L79, A80, L86, L100
7×10^{-5} min$^{-1} < k_{ex} < 2 \times 10^{-4}$ min^{-1}	L28, L37, L58, V68, Y69, I70, S72, D82, G85, F99, I112, F122, V123, A143, I144, L145, F146, L147
2×10^{-4} min$^{-1} < k_{ex} < 1 \times 10^{-2}$ min^{-1}	K26, C30, N32, F36, G43, T44, V45, D46, G47, T48, I56, Q57, Q59, E67, K71, L87, Y88, G89, S90, C97, L98, E101, R102, N109, T110, Y111, S113, K114, W121, G124, L125, K126, S130, K132, G134, R136, L149
$k_{ex} > 1 \times 10^{-2}$ min^{-1}	H35, D53, H55, Q77, S61, D84, E104, Y108, G129, T137, V151
residues which disappeared in the first 20 min of exchange	K24, S31, G33, G34, D42, R49, D50, R51, S52, Q54, L60, A62, E63, S64, V65, G66, T73, E74, T75, G76, M81, T83, Q91, T92, N94, E95, E96, L103, H107, K115, H116, A117, E118, K119, N120, K127, N128, C131, R133, H138, Y139, G140, K142, S152, S153, D154

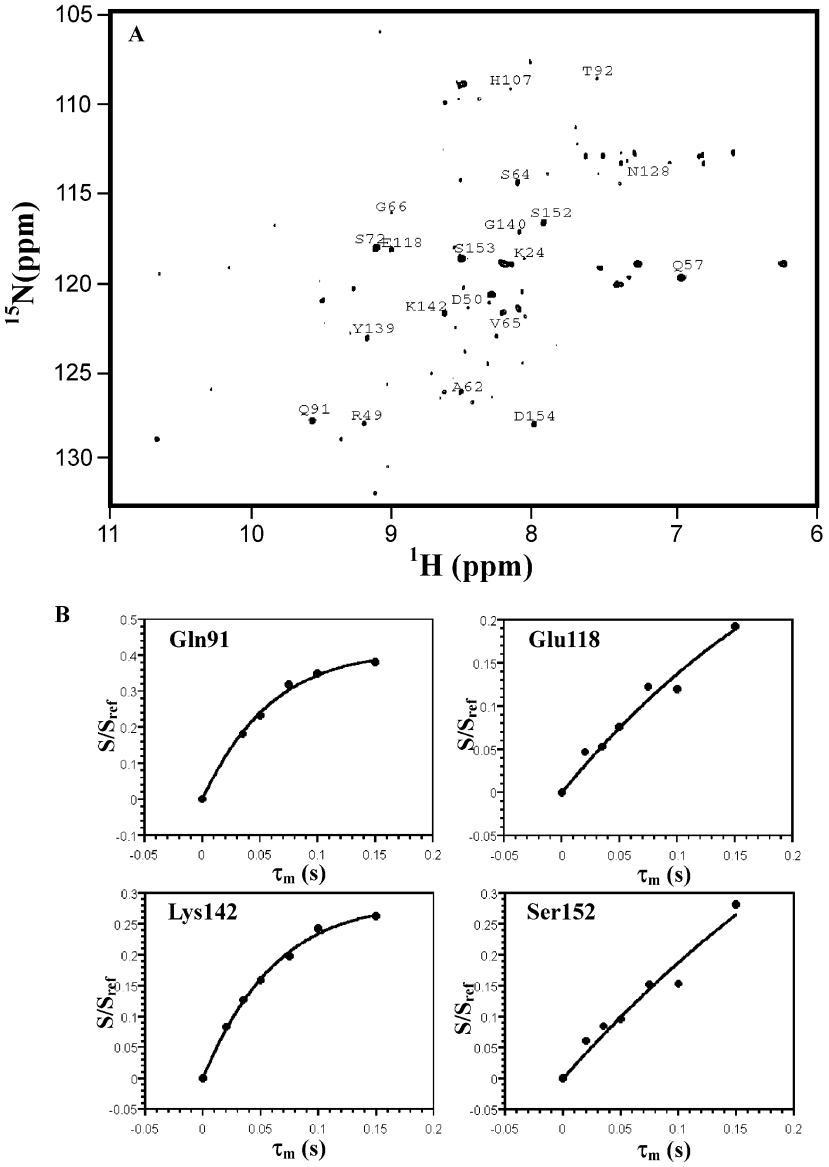

FIGURE 4: (A) ^{1}H−^{15}N clean SEA-HSQC spectra of hFGF-1. The clean SEA-HSQC spectrum was acquired with a mixing time of 20 ms. Most of the 46 cross-peaks corresponding to fast-exchanging, solvent-exposed amide protons could be detected in the spectra. The labeled cross-peaks represent the fast-exchanging amide protons whose exchange rates could be reliably calculated. (B) Relative intensity (S/S_{ref}) versus mixing time (τ_m) plot of selected residues (in hFGF-1) obtained from the clean SEA-HSQC experiments.

β-strand XI (20 231 ± 194) (Figure 5). Among the 12 β-strands in the protein, the average protection of β-strand XI is the least, and this observation is consistent with the three-dimensional structure of hFGF-1 derived using NMR spectroscopy (*34*). The β-trefoil structure of hFGF-1 in solution is shown to possess 11 β-strands instead of 12 β-strands as in the crystal structures (*31*, *34*). The observed discrepancy between the solution and crystal structures could be rationalized by the high conformational flexibility (as indicated by low average protection factor) of residues in β-strand XI in solution, which in turn eludes observation of intramolecular NOEs (characterizing β-strand XI). The crystal structure of the ternary complex of hFGF-1/heparin/hFGF-1 receptor (*27*), and ^{15}N chemical shift perturbation data (*41*) obtained upon titration of hFGF-1 with structural analogues of heparin (such as sucrose octasulfate), show that

Table 2: Hydrogen−Deuterium-Exchange Rates Measured by Clean SEA-HSQC Experiments

	k_{ex} (min^{-1})		k_{ex} (min^{-1})		k_{ex} (min^{-1})
K24	28.1 ± 0.5	G66	121.9 ± 8.8	Y139	220.1 ± 2.4
R49	150.4 ± 7.1	Q91	422.1 ± 9.9	G140	207.4 ± 2.9
D50	56.2 ± 2.5	T92	91.4 ± 0.4	K142	278.0 ± 0.5
A62	60.6 ± 1.4	H107	124.5 ± 5.7	S152	127.3 ± 3.0
S64	50.3 ± 2.9	E118	98.5 ± 1.8	S153	1429.1 ± 21.7
V65	86.8 ± 2.5	N128	38.6 ± 1.0	D154	101.1 ± 5.1

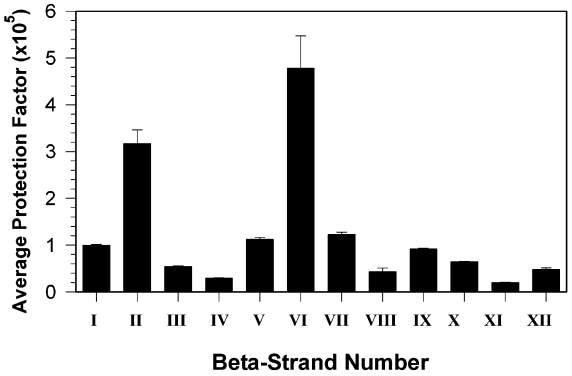

FIGURE 5: Average protection factors of various β-strands in hFGF-1. β-Strands II and VI appear to constitute the stable core of the protein. Residues in β-strand XI exhibit relatively low protection factors and constitute a portion of the heparin binding domain.

the segment comprising residues 126−142 in hFGF-1 constitutes the heparin binding site. In this context, the low protection factors of most of the residues in β-strand XI (Ser130 to Gly134, Figure 5) and the two adjoining loops (Lys127 to Gly129 and Arg136 to Lys142) bear functional significance. The high flexibility of residues (in the heparin binding region) might favor complex formation with the proteoglycan (heparin sulfate) by lowering the free energy barrier.

There are significant differences in the average protection factors of the various β-strands. Among the various β-strands in the protein, β-strand VI exhibits the greatest average protection factor (478 405 ± 68 866, Figure 5). Ala80, in β-strand VI, shows an extraordinarily high protection factor. The amide proton of Ala80 is involved in a hydrogen bond with Tyr88, located in β-strand VII (Figure 6). The presence of this hydrogen bond stabilizes the hydrophobic cluster (comprising residues in β-strands VI and VII), with Ala80 located in the middle of the nonpolar core. This aspect might accounts for the unusually high protection of the amide proton of Ala80 against H/D exchange (Figure 7A). Similarly, the high average protection factor of residues in β-strand II could be rationalized by the presence of a network of hydrogen bonds between Leu37NH and Leu28CO, and between Leu149NH and Leu27CO (Figures 5 and 6). These hydrogen bonds forge a hydrophobic patch consisting of Leu27, Leu28, Tyr29, Phe36, Leu37, Ile39, Leu147, and Leu149. The tight packing of residues in β-strand II renders their amide protons resistant to solvent exchange (Figure 6). The β-hairpin structure stabilized by two hydrogen bonds, Arg38NH−Asp46CO and Ile39NH−Lys26CO, effectively protects the amide protons of residues in β-strand II (Figures 6 and 7) from the solvent and accounts for their high protection factors. In summary, the analysis of the protection factor data has helped in the identification of structural interactions that contribute to the conformational stability of hFGF-1.

The Hydrogen−Deuterium-Exchange Mechanism. The free energy change (ΔG_{ex}) estimated from the H/D exchange, in principle, is expected to be equal to or lower than the free energy change of unfolding [$\Delta G(D_2O)$] deduced from the equilibrium unfolding experiments (using steady-state fluorescence/far-UV CD spectroscopy). However, the majority of the slowest exchanging protons in hFGF-1 exhibit ΔG_{ex} values larger than the $\Delta G(D_2O)$ value (5.00 ± 0.09 kcal·mol^{-1}) estimated from equilibrium unfolding experiments. Similar findings have been reported for amide protons of *Saccharomyces cerevisiae* oxidized iso-1-cytochrome *c* (*42*), cytochrome *c* (*43*), proteins G B1 and B2 domains (*43*), ovomucoid third domain (*44*), cardiotoin analogue III (*45*), ribonuclease T1 (*46*), and also RNase A under different conditions (*47*, *48*). The possible sources of discrepancy could be (1) increased stability of protein in D_2O (*21*) used in H/D-exchange experiments, (2) exchange of the amide protons occurring by the EX1 mechanism instead of the EX2 mechanism (*49*), (3) *cis*−*trans*-proline isomerization in the protein (*24*), or (4) the presence of residual structure(s) in the unfolded state(s). In the case of hFGF-1, the first three possibilities can be ruled out. Proteins have been shown to be stabilized in D_2O (*14*). However, as the equilibrium unfolding experiments in hFGF-1 have been performed in D_2O, the ΔG_u values (obtained from equilibrium unfolding experiments) are directly comparable with the ΔG_{ex} values (obtained from amide proton-exchange measurements). This aspect rules out the possibility that the observed discrepancy is due to stabilization of the protein in D_2O. The exchange rates of amide protons were measured at two different pDs (pD 6.0 and pD 7.0). The slope of the log k_{ex}(pD 6.0) versus log k_{ex}(pD 7.0) plot is observed to be linear, with a slope of about 0.9. These results clearly suggest that the slow-exchanging amide protons in hFGF-1 exchange by the EX2 mechanism. If exchange were to occur by EX1 (resulting in overestimation of ΔG_{ex}), the exchange rates of the amide protons would be expected to be pH-independent. The third possibility of *cis*−*trans*-proline isomerization contributing to the observed discrepancy (between ΔG_{ex} and ΔG_u) could be discounted because all the six prolines in the native state of hFGF-1 are shown to be in the trans conformation (*34*). In addition, our recent study on the kinetics of refolding of hFGF-1 (*30*) revealed that refolding of the protein from the denatured state(s) does not involve *cis*−*trans*-proline isomerization. Although at the present juncture we do not have direct concrete experimental evidence, we are inclined to believe that the observed discrepancy between the ΔG_{ex} and ΔG_u values (in hFGF-1) stems from the presence of residual structure(s) in the unfolded state(s). Residual structure(s) (in unfolded state(s)), in general, would imply that the values of k_{rc} which are calculated on the basis of poly-DL-alanine reference states are overestimates for the actual chemical exchange rates. An overestimation of k_{rc} could result in higher ΔG_{ex}. It should be mentioned that the presence of compact unfolded state(s) in the protein (hFGF-1) under native conditions is also consistent with our protection factor data on the slow-exchanging amide protons (Table 1, Figure 7). In principle, the amide protons of a fully unfolded protein should have identical protection factors. However, we observe that the protection factors for the slow-exchanging

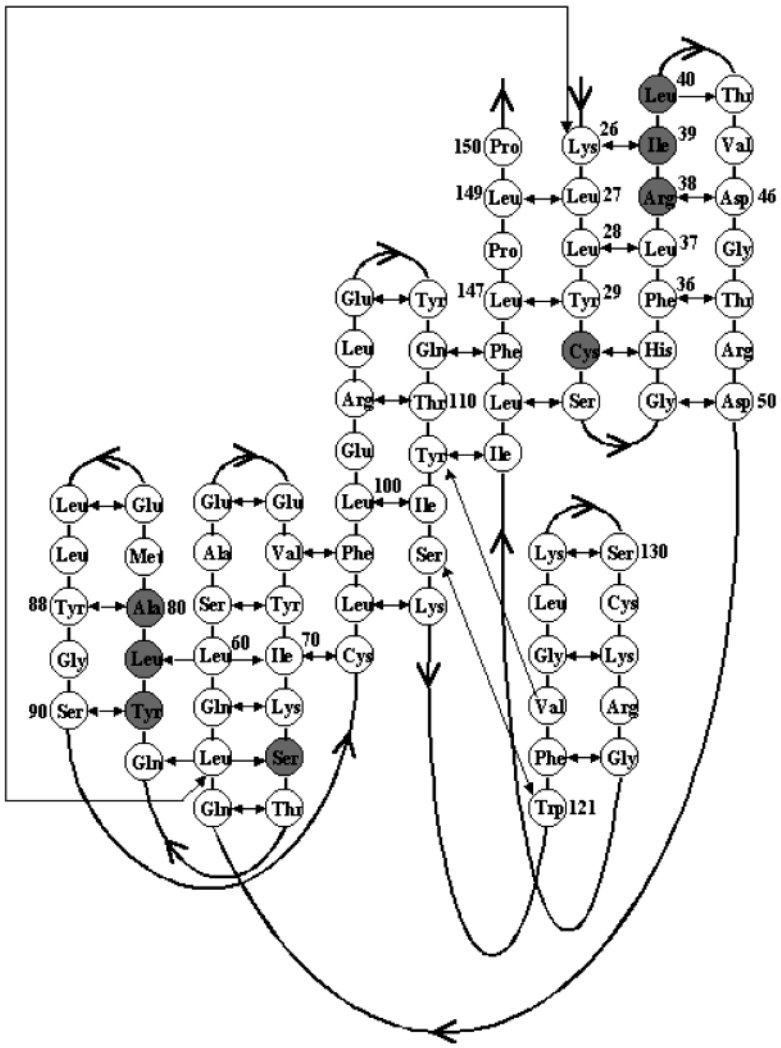

FIGURE 6: Main-chain hydrogen bonding of hFGF-1, showing the positions of the slowly exchanging amides ($P > 300\,000$, indicated in gray). The arrowheads indicate the direction of the polypeptide chain from the N- to C-terminal end. The hydrogen-bonding pattern shown in this figure is in accordance with the solution structure of hFGF-1 published by Pineda-Lucena et al. (*33*).

amide protons in hFGF-1 cover a range of about 100-fold, suggesting the presence of residual structure(s) in the (compact) unfolded states. In addition, recent NMR data acquired in our laboratory (Yu et al., unpublished data) on the pH-denatured state(s) of hFGF-1 suggest the presence of localized regions of residual structure.

Correlation between Temperature Coefficient and Protection Factor. Amide proton temperature coefficient ($\Delta\delta/\Delta T$) measurements are useful to probe solvent accessibilities of residues and also to monitor the conformational changes accompanying a temperature-induced unfolding process (*50*, *51*). The information obtained from temperature coefficient measurements is complementary to that gained from hydrogen−deuterium-exchange studies. In addition, temperature coefficients are ideal measures of hydrogen bonding, since they are not very sensitive to pH (*52*), local structure fluctuations (*53*), and the presence of a hydrogen-bonded carbonyl group that has the same peptide bond as the amide proton whose exchange is being measured (*54*). Amide protons show marked changes in their chemical shift values with temperature. Amide protons which are not hydrogen bonded and exposed to the solvent show larger changes in the chemical shift values than those which are involved in hydrogen bonding in the protein molecule. In general, the magnitudes of the temperature coefficients estimate are inversely related to the relative stability of the residue in the protein (*50*, *51*). The temperature coefficients of amide protons serve as indicators for hydrogen bonding, and in general, values more positive than −4.5 ppb/K are indicative of the involvement of the amide protons in intramolecular hydrogen bonding (*50*, *51*).

The chemical shifts of most of the amide protons of hFGF-1 change linearly with temperature (in the temperature range of 288.5−306 K). Thirty out of the 114 residues for which the temperature coefficients could be estimated show temperature coefficient values more negative than −4.5 ppb/K (Figure 7B). Most of these residues are located in the unstructured loop regions of the protein. Few residues located in structured regions such as Ser61 (β-strand IV), Ala80 (β-strand VI), and Leu86 (β-strand VII) show amide proton temperature coefficient values more positive than −0.9 ppb/K (Figure 7B). Interestingly, Ala80 ($P = 1.45 \times 10^6$) and Leu86 ($P = 1.66 \times 10^5$) exhibit exceptionally high protection against exchange (Figure 7B). In contrast, the amide proton of Ser61 exchanges out within 20 min of initiation of exchange (in D_2O). Although the amide proton of Ser61 is hydrogen bonded to the carbonyl group of Tyr69, it is located on the surface of the hFGF-1 molecule, thus

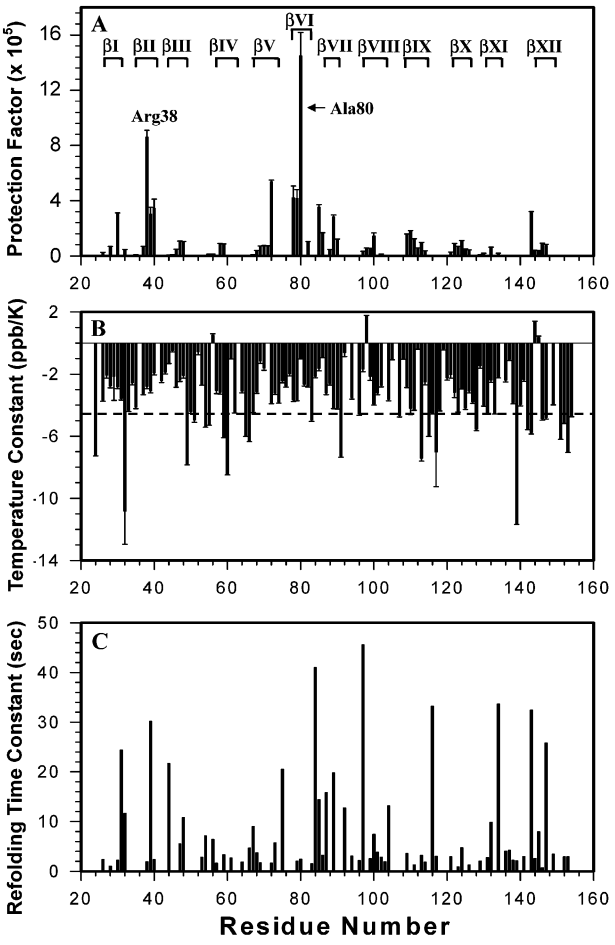

FIGURE 7: Correlation between the protection factor (A), temperature coefficient (B), and refolding time constant (C) of residues in hFGF-1. Amide protons of residues such as Arg38 and Ala80 show exceptionally large protection values ($P > 850\,000$). In general, residues that are highly protected display more positive temperature coefficient values. However, the correlation is found to break down when hydrogen-bonded amide protons are located on the solvent-accessible surface of the protein. The temperature coefficient value of −4.5 ppb/K (broken line) is believed to be the upper limit for hydrogen bonding. (C) Refolding time constants of residues in hFGF-1. The residues strongly protected against exchange do not correspond to the residues that exhibit small time constant values.

rendering it vulnerable to rapid exchange with the solvent. At the present juncture, we do not have a rational explanation for the unusual temperature coefficient value exhibited by Ser61. However, the high density of hydrogen bonds among residues in the vicinity of Ser61 might restrict the local thermal fluctuations and consequently decrease the temperature-induced changes in the amide proton (of Ser61) chemical shift.

^{15}N spin relaxation measurements characterizing the backbone dynamics of hFGF-1 revealed that 13 residues exhibit conformational exchange (R_{ex}) values larger than 4 s^{-1} (*45*). R_{ex} values are indicators of line broadening due to conformational exchange in the milli- to microsecond time scale regime. The residues undergoing slow conformational exchange are found distributed uniformly on the structure of hFGF-1. As most of the residues showing larger R_{ex} values are located in close proximity to proline residues, the slow conformational motions observed in the free form of hFGF-1 were attributed to *cis*−*trans*-proline isomerization (*45*). Baxter et al. (*51*) recently demonstrated that temperature coefficient measurements could be reliable probes for detecting conformational exchange in proteins. Chemical shifts of residues undergoing slow conformational exchange are shown to display curved temperature dependences. The curvature in the temperature coefficient profiles suggest that the amide proton can access more than one conformational state, the relative free energies of which vary as a function of temperature (*51*). Among the 13 residues with high R_{ex} values, only the chemical shift of the amide proton of Leu98 shows curved temperature dependences (data not shown). The observed discrepancy could be because the temperature-dependent amide proton chemical shifts of the amide protons were monitored only up to 306 K, wherein the population of residues accessing excited alternative conformational state-(s) (that are in low free energy relative to the ground state) is small. The temperature-dependent amide proton chemical shifts in hFGF-1 could not be monitored beyond 310 K due to problems arising from protein aggregation.

The average temperature coefficient and average protection values of the various β-strands in hFGF-1 show a reasonably good agreement. β-Strands II, V, VI, and VII, which exhibit high protection against H/D exchange, show low average amide proton temperature coefficient values (Figure 7B, average $NH\Delta\delta/\Delta T$ values more positive than −3.18 ppb/K). Similarly, residues in β-strands IV and IX, which exchange fast, show average amide proton temperature coefficient values less positive than −3.5 ppb/K. In contrast, the amide protons of residues in β-strands III and VIII, which are highly susceptible to H/D exchange, show exceptionally low average amide proton temperature coefficient values ($\Delta\delta/\Delta T$ more positive than −2.5 ppb/K, Figure 7B). Such discrepancies between amide-exchange rates and temperature coefficients have been reported in a number of studies (*55*−*57*). In contrast to exchange rates, which are strongly correlated to surface exposure, amide proton temperature coefficients are not strongly influenced by solvent accessibility (*51*, *56*, *57*).

Is There a Relationship between Hydrogen Exchange and Events in the Folding Pathway of hFGF-1? Woodward and co-workers proposed a few years ago that the protein folding core can be a subset of the slow-exchanging core (*58*, *59*). This essentially means that the folding pathway approximates the reverse order of the native-state hydrogen-exchange rates; i.e., the last hydrogen to exchange might identify the first part of the protein to fold—"last out, first in". This correlation was found to be valid to a large extent in five proteins: bovine pancreatic trypsin inhibitor (*58*), lysozyme (*60*), cytochrome *c* (*61*), RNase T_1 (*51*), and cardiotoxin analogue III (*62*). Recently, Lacroix et al. (*63*), comparing the equilibrium amide proton-exchange kinetics with the events in the folding pathway of chemotatic protein (CheY) from *Escherichia coli* using quenched-flow H/D exchange, showed that the highest protection from hydrogen exchange is a part of the folding nucleus. However, Fersht and co-workers, based on their studies on barnase (*64*, *65*) and chymotrypsin inhibitor 2 (*66*, *67*), showed that there is no obvious relationship between hydrogen exchange at equilibrium and the chronology of events in the folding pathways (*68*). They found that some protons belonging to regions that are formed early in the folding reaction do not belong to the group of slowest exchanging protons. In fact, tertiary structure inter-

actions, known to be formed late during the folding pathway, involved some of the slowest exchange protons in these proteins (*68*).

We recently investigated the structural events in the refolding pathway of hFGF-1 using a variety of techniques, including quenched-flow hydrogen−deuterium exchange (*69*). Thus, comparison of the results of the native-state hydrogen-exchange kinetics obtained in the present study and the quenched-flow hydrogen−deuterium (H/D)-exchange data provides a good opportunity to examine whether there exists a relationship between slowly exchanging regions and the folding nucleus of proteins. Complete refolding of hFGF-1 occurs in about 100 s. Quenched-flow H/D-exchange data revealed that the first structural event observed during the refolding of hFGF-1 is the generation of the basic β-trefoil framework provided by the simultaneous formation of β-strands I, IV, IX, and X. However, the equilibrium H/D-exchange data (acquired in the present study) show that all four of these β-strands (I, IV, IX, and X) display smaller protection factors (Figure 7A,C). On the other hand, β-strands II and VI, which exhibit exceptionally large average protection factor values, are observed to be formed late during the refolding of the protein. Similarly, Arg38, Ser72, and Ala80, which are highly protected from exchange ($P > 500\,000$), exhibit relatively large refolding time constant values (70). Therefore, it appears that, at least in hFGF-1, the protein folding core does not appear to a subset of the slow-exchange core.

FGF-Receptor Interaction Sites. Two classes of cell surface receptors have been identified for FGFs: the high-affinity and low-affinity receptors (*27*, *64*). The high-affinity receptors are composed of an extracellular ligand binding domain that contains three immunoglobulin-like domains (D1, D2, and D3), a single transmembrane helix, and a cytoplasmic domain that has tyrosine kinase activity (*27*). The low-affinity receptors include proteoglycans such as heparin/heparan sulfate. It is believed that heparin-induced dimerization of the ligand (hFGF-1) and the receptor is crucial for the mitogenic activity elicited by hFGF-1.

Investigation of the dynamic motions in proteins can yield useful information on ligand−receptor interaction. In general, the mechanisms of receptor interaction sites on the ligand are expected to be relatively more flexible than other portions (of the ligand molecule). The higher conformational flexibility is proposed to have significant effect(s) on the thermodynamics and kinetics of ligand−receptor binding. The higher flexibility of residues (in the ligand) involved in receptor binding is believed to increase the solvent-accessible surface area and consequently increase the probability of binding and optimization (decrease in the free energy of interaction) of the ligand to the receptor (*2*). In this context, it would be interesting to examine if the dynamics data obtained on hFGF-1 (in the present study) bears any physiological relevance.

FGF-1 is known to interact extensively with the D2 and D3 as well as the linker between the two domains (*64*). FGF-1 interacts with the D2 domain through hydrophobic and hydrogen bond contacts. The residues located in the βI/βII turn, the βIII/βIV loop, the βX/βXI loop, and the C-terminal residues are proposed to be the primary contact sites between FGF-1 and the D2 domain (*64*). With the exception of residues in β-strand IX, and Asp53, His55, and Ile56 (in the βIII/βIV loop), the other portions of the ligand (hFGF-1) molecule involved in receptor binding display very weak protection against exchange. For example, Gly34 (in βI/βII turn), Lys127, Asn128, and Gly129 (in βX/βXI loop), and Val151, Ser152, and Asp154 exchange out within the first 20 min of exchange, reflecting high backbone flexibility of these residues (Table 1). Similarly, residues in β-strands VIII and XII (Cys97−Leu103), which are shown to play a crucial role in the interaction of FGF-1 with the linker between the D2 and D3 domains (of the receptor), exchange rapidly with the solvent (D_2O, Figure 7A). In addition, the amide proton of Glu101 (in β-strand VIII), that is highly conserved in all FGFs and shown to participate in crucial hydrogen bond interaction with the D2 domain of the receptor, exchanges rapidly with the solvent (Figure 7A). Therefore, it appears that the recognition and kinetics of the FGF-1/receptor interaction are primarily governed by residues located in the region(s) of the ligand (FGF-1) exhibiting high backbone flexibility. The structured regions of the FGF-1 molecule seem to be involved in the stabilization of the ligand−receptor complex. A detailed study using site-specific mutants is currently underway to validate some of the proposals made in this study.

REFERENCES

1. Ishima, R., and Torchia, D. A. (2000) *Nat. Struct. Biol. 7*, 740−743.
2. Kay, L. E. (1998) *Nat. Struct. Biol. 5*, 513−517.
3. Feher, V. A., and Cavanagh, J. (1999) *Nature 400*, 289−293.
4. Stone, M. J. (2001) *Acc. Chem. Res. 34*, 379−388.
5. Bracken, C., Carr, P. A., Cavanagh, J., and Palmer, A. G., III. (1999) *J. Mol. Biol. 285*, 2133−2146.
6. Hodsdon, M. E., and Cistola, D. P. (1997) *Biochemistry 36*, 2278−2290.
7. Ehrhardt, M. R., Urbauer, J. L., and Wand, A. J. (1995) *Biochemistry 34*, 2731−2738.
8. Frauenfelder, H., Sligar, S. G., and Wolynes, P. G. (1991) *Science 254*, 1598−1603.
9. Cavanagh, J., and Akke, M. (2000) *Nat. Struct. Biol. 7*, 11−13.
10. Palmer, A. G., III. (1997) *Curr. Opin. Struct. Biol. 7*, 732−737.
11. Daiye, K. T., Wagner, G., and Lefevre, J. F. (1996) *Annu. Rev. Phys. Chem. 47*, 243−282.
12. Jardetzky, O., and Lefevre, J. F. (1994) *FEBS Lett. 338*, 246−250.
13. Englander, S. W., and Kallenbach, N. R. (1983) *Q. Rev. Biophys. 16*, 521−655.
14. Englander, S. W., and Mayne, L. (1992) *Annu. Rev. Biophys. Biomol. Struct. 21*, 243−265.
15. Baldwin, R. L. (1993) *Curr. Opin. Struct. Biol. 3*, 84−91.
16. Palmer, A. G., III. (1993) *Curr. Opin. Biotechnol. 4*, 385−391.
17. Clarke, J., and Itzaki, L. S. (1998) *Curr. Opin. Struct. Biol. 8*, 112−118.
18. Arrington, G. B., and Robertson, A. D. (2000) *J. Mol. Biol. 296*, 1307−1317.
19. Bai, Y., Sosnick, T. R., Mayne, L., and Englander, S. W. (1995) *Science 269*, 192−197.
20. Li, R., and Woodward, C. (1999) *Protein Sci. 8*, 1571−1590.
21. Englander, S. W., Mayne, L., Bai, Y., and Sosnick, T. R. (1997) *Protein Sci. 6*, 1101−1109.
22. Englander, S. W., Sosnick, T. R., Englander, J. J., and Mayne, L. (1996) *Curr. Opin. Struct. Biol. 6*, 18−23.
23. Kim, K. S., and Woodward, C. (1993) *Biochemistry 32*, 9609−9613.
24. Bai, Y., Milne, J. S., Mayne, L., and Englander, S. W. (1994) *Proteins: Struct., Funct. Genet. 20*, 4−14.
25. Bai, Y., Englander, J. J., Mayne, L., Milne, J. S., and Englander, S. W. (1994) *Methods Enzymol. 259*, 344−356.
26. Sivaraman, J., Arrington, C. B., and Robertson, A. D. (2001) *Nat. Struct. Biol. 8*, 331−333.

27. Schlessinger, J., Plotnikov, A. N., Ibrahami, O. A., Eliseenkova, A. V., Yeh, B. K., Yayon, A., Linhardt, R. J., and Mohammadi, M. (2000) *Mol. Cell 6*, 743−750.
28. Mach, H., and Middaugh, C. R. (1995) *Biochemistry 34*, 9913−9920.
29. Chi, Y. H., Kumar, T. K. S., Wang, H. M., Ho, M. C., Chiu, I. M., and Yu, C. (2001) *Biochemistry 40*, 7746−7753.
30. Samuel, D., Kumar, T. K. S., Srimathi, T., Hsieh, H. C., and Yu, C. (2000) *J. Biol. Chem. 275*, 34968−34975.
31. Zhu, X., Hsu, B. T., and Rees, D. C. (1993) *Structure 1*, 27−34.
32. Blaber, M., Disalvo, J., and Thomas, K. A. (1996) *Biochemistry 35*, 2086−2094.
33. Pineda-Lucena, A., Jimenez, M. A., Lozano, R. M., Nieto, J. L., Santoro, J., Rico, M., and Gimenez-Gallego, G. (1996) *J. Mol. Biol. 264*, 162−178.
34. Ogura, K., Nagata, H., Habushi, H., Kimata, K., Tate, S., Ravera, M. W., Jaye, M., Schlessinger, J., and Inagaki, F. (1999) *J. Biomol. NMR 13*, 11−24.
35. Chi, Y. H., Kumar, T. K. S., Chiu, I. M., Yu, C. (2002) *J. Biol. Chem. 277*, 34941−34948.
36. Dyson, H. J., Rance, M., Honghton, R. A., Lerner, R. A., and Wright, P. E. (1988) *J. Mol. Biol. 201*, 161−200.
37. Lin, D., Sze, K. H., Cui, Y. F., and Zhu, G. (2002) *J. Biomol. NMR 23*, 317−322.
38. Hwang, T. L., van Zijl, P. C. M., and Mori, S. (1998) *J. Biomol. NMR 11*, 221−226.
39. Lozano, R. M., Pineda-Lucena, A., Gonzalez, C., Jimenez, M. A., Cuevas, P., Redono-Horcaju, M., Sanz, J. M., Rico, M., and Gimenez-Gallego, G. (2000) *Biochemistry 39*, 4982−4993.
40. Burke, C. J., Volkin, D. B., Mach, H., and Middaugh, C. R. (1993) *Biochemistry 32*, 6419−6426.
41. Chi, Y. H., Kumar, T. K. S., Chiu, I. M., and Yu, C. (2000) *J. Biol. Chem. 275*, 39444−39450.
42. Marmorino, J. L., Auld, D. S., Betz, S. F., Doyle, D. F., Young, G. B., and Pielak, G. J. (1993) *Protein Sci.* 2, 1966−1974.
43. Orban, J., Alexander, P., Bryan, P., and Khare, D. (1995) *Biochemistry 34*, 15291−15300.
44. Swint-Kruse, L., and Robertson, A. D. (1996) *Biochemistry 35*, 171−180.
45. Sivaraman, T., Kumar, T. K. S., and Yu, C. (1999) *Biochemistry 38*, 9899−9905.
46. Mullins, L. S., Pace, C. N., and Raushel, F. M. (1997) *Protein Sci. 6*, 1387−1395.
47. Mayo, S. L., and Baldwin, R. L. (1993) *Science 262*, 873−876.
48. Wang, A., Robertson, A. D., and Bolen, D. W. (1995) *Biochemistry 34*, 15096−15104.
49. Perrett, S., Clarke, J., Hounslow, A. M., and Fersht, A. R. (1995) *Biochemistry 34*, 9288−9298.
50. Baxter, N. J., and Willamson, M. P. (1997) *J. Biomol. NMR 9*, 359−369.
51. Baxter, N. J., Hosszu, L. L., Waltho, J. P., and Williamson, M. P. (1998). *J. Mol. Biol. 284*, 1625−1639.
52. Pedersen, T. G., Sigurskjold, B. W., Andersen, K. V., Kjaer, M., Poulsen, C. M., Dobson, C. M., and Redfield, C. (1991) *J. Mol. Biol. 218*, 413−426.
53. Woodward, C., Simon, I., and Tuchsen, E. (1982) *Mol. Cell. Biochem. 48*, 135−160.
54. Persin, C. L., Dwyer, T. J., Rebek, J., and Duff, R. J. (1990) *J. Am. Chem. Soc. 112*, 3122−3125.
55. Delepierre, M., Larvor, M. P., Baleux, F., and Goldberg, M. E. (1991) *Eur. J. Biochem. 201*, 681−693.
56. Andersen, N. H., Chen, C., Marchner, T. M., Krystek, S. R., Jr, and Bassolino, D. A. (1992) *Biochemistry 31*, 1280−1295.
57. Skalicky, J. J., Selsted, M. E., and Pardi, A. (1994) *Proteins 20*, 52−67.
58. Kim, K. S., Fuchs, J. A., and Woodward, C. K. (1993) *Biochemistry 32*, 9600−9608.
59. Woodward, C. (1993) *Trends Biochem. Sci. 18*, 359−360.
60. Radford, S. E., Dobson, C. M., and Evans, P. A. (1992) *Nature 358*, 302−307.
61. Roder, H., Elove, G. A., and Englander, S. W. (1988) *Nature 335*, 700−704.
62. Sivaraman, T., Kumar, T. K. S., Lin, W. Y., Chang, D. K., and Yu, C. (1998) *J. Biol. Chem. 273*, 10181−10189.
63. Lacroix, E., Bruix, M., Lopez-Hernandez, E., Serrano, L., and Rico, M. (1997) *J. Mol. Biol. 271*, 472−487.
64. Clarke, J., Hounslow, A. M., Bycroft, M., and Fersht, A. R. (1993) *Proc. Natl. Acad. Sci. U.S.A. 90*, 9837−9841.
65. Clarke, J., and Fersht, A. R. (1996) *Fold. Des. 1*, 243−254.
66. Niera, J. L., Itzhaki, L. S., Otzen, D. E., Davis, B., and Fersht, A. R. (1997) *J. Mol. Biol. 270*, 99−110.
67. Itzhaki, L. S., Niera, J. L., and Fersht, A. R. (1997) *J. Mol. Biol. 270*, 89−98.
68. Clarke, J., Itzhaki, L. S., and Fersht, A. R. (1997) *Trends Biochem. Sci. 22*, 284−287.
69. Samuel, D., Kumar, T. K. S., Balamurugan, K., Lin, W. Y., and Yu, C. (2001) *J. Biol. Chem. 276*, 4134−4141.
70. Stauber, D. J., Digabnele, A. D., and Hendrickson, W. A. (2000) *Proc. Natl. Acad. Sci. U.S.A. 97*, 49−54.

BI026218A